

This work was written as part of one of the author's official duties as an Employee of the United States Government and is therefore a work of the United States Government. In accordance with 17 U.S.C. 105, no copyright protection is available for such works under U.S. Law. Access to this work was provided by the University of Maryland, Baltimore County (UMBC) ScholarWorks@UMBC digital repository on the Maryland Shared Open Access (MD-SOAR) platform.

Please provide feedback

Please support the ScholarWorks@UMBC repository by emailing scholarworks-group@umbc.edu and telling us what having access to this work means to you and why it's important to you. Thank you.

RESEARCH ARTICLE

10.1002/2017JD027768

Special Section:

Winter INvestigation of Transport, Emissions and Reactivity (WINTER)

Key Points:

- N_2O_5 loss rate is main factor controlling overnight NO_x loss via conversion to HNO_3 in power plant plumes
- Fate of organic nitrates is important factor in degree of overnight NO_x removal from power plant plumes
- Extremely low N_2O_5 loss rate constant and uptake coefficients observed in plume are below most prior observations

Supporting Information:

- Supporting Information S1
- Data Set S1

Correspondence to:

S. S. Brown,
steven.s.brown@noaa.gov

Citation:

Fibiger, D. L., McDuffie, E. E., Dubé, W. P., Aikin, K. C., Lopez-Hilfiker, F. D., Lee, B. H., ... Brown, S. S. (2018). Wintertime overnight NO_x removal in a Southeastern United States coal-fired power plant plume: A model for understanding winter NO_x processing and its implications. *Journal of Geophysical Research: Atmospheres*, 123, 1412–1425. <https://doi.org/10.1002/2017JD027768>

Received 21 SEP 2017

Accepted 1 JAN 2018

Accepted article online 5 JAN 2018

Published online 23 JAN 2018

Published 2018. This article has been contributed to by US Government employees and their work is in the public domain in the USA.

Wintertime Overnight NO_x Removal in a Southeastern United States Coal-fired Power Plant Plume: A Model for Understanding Winter NO_x Processing and its Implications

Dorothy L. Fibiger^{1,2} , Erin E. McDuffie^{1,3} , William P. Dubé^{1,2}, Kenneth C. Aikin^{1,2} , Felipe D. Lopez-Hilfiker⁴, Ben H. Lee⁴ , Jaime R. Green⁵, Marc N. Fiddler⁵, John S. Holloway¹, Carlena Ebben⁶, Tamara L. Sparks⁶ , Paul Wooldridge^{6,7}, Andrew J. Weinheimer⁸ , Denise D. Montzka⁸ , Eric C. Apel⁸ , Rebecca S. Hornbrook⁸ , Alan J. Hills⁸, Nicola J. Blake⁹ , Josh P. DiGangi¹⁰ , Glenn M. Wolfe^{10,11} , Solomon Bililign⁵, Ronald C. Cohen^{6,7} , Joel A. Thornton⁴ , and Steven S. Brown^{1,3} 

¹Chemical Sciences Division, Earth System Research Laboratory, National Oceanic and Atmospheric Administration, Boulder, CO, USA, ²Cooperative Institute for Research in Environmental Science, University of Colorado, Boulder, CO, USA, ³Department of Chemistry, University of Colorado, Boulder, CO, USA, ⁴Department of Atmospheric Sciences, University of Washington, Seattle, WA, USA, ⁵Department of Physics, North Carolina A&T State University, Greensboro, NC, USA, ⁶Department of Chemistry, University of California, Berkeley, CA, USA, ⁷Department of Earth and Planetary Science, University of California, Berkeley, CA, USA, ⁸Atmospheric Chemistry Observations & Modeling Laboratory, National Center for Atmospheric Research, ⁹Department of Chemistry, University of California, Irvine, CA, ¹⁰NASA Langley Research Center, Hampton, VA, ¹¹NASA Goddard Space Flight Center, Greenbelt, MD

Abstract Nitric oxide (NO) is emitted in large quantities from coal-burning power plants. During the day, the plumes from these sources are efficiently mixed into the boundary layer, while at night, they may remain concentrated due to limited vertical mixing during which they undergo horizontal fanning. At night, the degree to which NO is converted to HNO_3 and therefore unable to participate in next-day ozone (O_3) formation depends on the mixing rate of the plume, the composition of power plant emissions, and the composition of the background atmosphere. In this study, we use observed plume intercepts from the Wintertime INvestigation of Transport, Emissions and Reactivity campaign to test sensitivity of overnight NO_x removal to the N_2O_5 loss rate constant, plume mixing rate, background O_3 , and background levels of volatile organic compounds using a 2-D box model of power plant plume transport and chemistry. The factor that exerted the greatest control over NO_x removal was the loss rate constant of N_2O_5 . At the lowest observed N_2O_5 loss rate constant, no other combination of conditions converts more than 10% of the initial NO_x to HNO_3 . The other factors did not influence NO_x removal to the same degree.

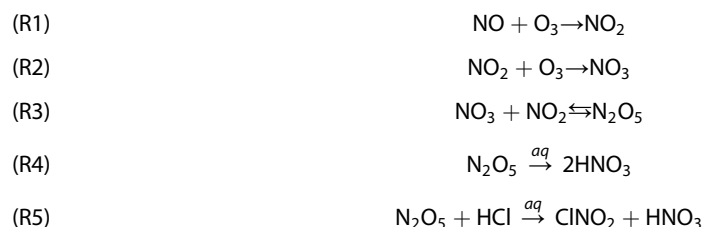
1. Introduction

Nitric oxide (NO) and nitrogen dioxide (NO_2), together known as NO_x , play a key role in ozone (O_3) production. O_3 is a major component of photochemical smog and can be hazardous to human health and vegetation. During the day, NO and NO_2 are rapidly interconverted, and in the presence of oxidation of volatile organic compounds (VOCs), this interconversion gives a net production of O_3 . At night, NO_x chemistry becomes an O_3 sink and NO_x can be removed from the atmosphere by conversion to HNO_3 through the reaction sequence below.

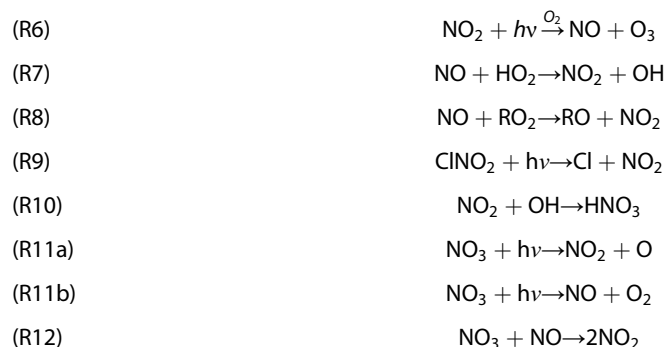
Electricity generation from power plants is a major source of NO_x to the atmosphere. In the United States in 2015, power plants emitted 1.61 Tg of NO_x (all referenced in this paper measured as NO_2), accounting for 14% of nationwide NO_x emissions, down from a maximum of 26% in 1993 (<https://www.epa.gov/air-emissions-inventories/air-pollutant-emissions-trends-data>). Trends in other regions differ substantially from the U.S. In China, for example, power plant NO_x emissions are significantly higher. In 2010, 8.29 Tg of NO_x were emitted from Chinese power plants (a 335% increase from 1990) (Liu et al., 2015), while in the U.S., it was 2.23 Tg. Thus, understanding the fate of power plant NO_x emissions is important on both a regional and global basis.

Emissions from power plants are rapidly mixed into convective boundary layers during the day, resulting in rapid dilution (Ryerson et al., 1998). At night, the buoyant emissions from power plant stacks can reach

altitudes within the residual layer (i.e., several hundred meters above ground level). Under stable conditions within the residual layer (increasing potential temperature with altitude), vertical mixing can be restricted (Brown et al., 2007, 2012; Luria et al., 2008; Zaveri et al., 2010). Rather, the plumes mix primarily in the horizontal, resulting in shallow “fanning” plumes (Turner, 1994) up to several km in width, but vertically only tens to a few hundreds of meters deep. The combination of large NO_x emissions and inefficient mixing can rapidly lead to complete removal of O₃ within nighttime plumes from (R1), limiting further oxidative chemistry ((R2)–(R5)). If NO_x emissions are low enough and/or mixing background O₃ into the plume during transport is efficient, then nighttime NO_x chemistry proceeds according to (R1)–(R5).



If, overnight, NO_x is converted to HNO₃ ((R4) and (R5)), usually a terminal product of NO_x oxidation, it cannot participate in O₃ chemistry the following day through (R1) and (R6)–(R8). The degree to which NO_x is converted to HNO₃ overnight in a power plant plume depends on several factors including the mixing rate of the plume with background air, the NO emissions from the plant, and the O₃ concentration in the background. If, in contrast, NO_x remains unreacted or is converted to N₂O₅ or ClNO₂, it is not removed from the system, rejoins the NO/NO₂ cycle, and participates in O₃ formation and/or longer-range transport. After sunrise, N₂O₅ thermally decomposes to form two NO_x molecules ((R3) backward reaction, followed by (R11a) or (R11b)), while ClNO₂ undergoes photolysis to form NO₂ and a Cl radical (R9). During the day, NO_x can be converted to HNO₃ through hydroxyl radical (OH) chemistry (R10), but N₂O₅ chemistry is unimportant because N₂O₅ thermally decomposes to NO₂ and NO₃ ((R3) backward reaction) and the NO₃ produced is quickly photolyzed back to NO₂ (R11a), NO (R11b) or reacts rapidly with NO (R12).



Nighttime chemistry is more important to understanding NO_x budgets in the winter than in summer due to longer duration of night and reduced daytime photochemical activity. Wintertime atmospheric chemistry, however, is generally less well studied than summertime. While nighttime NO_x chemistry has been studied in warm conditions (Atkinson et al., 1986; Brown et al., 2004; Brown & Stutz, 2012; McLaren et al., 2004), wintertime observations are far more limited (Brown et al., 2013; Riedel et al., 2013; Wagner et al., 2013). There has been significant work on nitrogen chemistry in power plant plumes in the summer both during the day (Hegg et al., 1977; Hewitt, 2001; Ryerson et al., 2001) and at night (Brown & Stutz, 2012; Luria et al., 2008; Zaveri et al., 2010), but lower temperatures and longer nights will affect the chemistry of power plant plumes in winter.

In this study, we use observations of the plume from the Harlee Branch power plant in Putnam County, GA, during the Wintertime INvestigation of Transport, Emissions, and Reactivity (WINTER) campaign to constrain parameters related to overnight chemistry. These parameters are included in a 2-D box model to examine overnight conversion of NO to HNO₃ and organic nitrates.

2. Methods

The WINTER campaign was conducted in February and March 2015 on the National Science Foundation/National Center for Atmospheric Research (NSF/NCAR) C-130. Based out of NASA Langley in Hampton, VA, the campaign consisted of 13 research flights over the eastern United States and the Atlantic Ocean. We primarily present data from a flight on 7 March over Georgia, downwind of the Atlanta metro area.

2.1. Instrumentation

The aircraft was instrumented with a comprehensive set of trace gas and aerosol measurements for the campaign. Aerosol surface area was calculated from a passive cavity aerosol spectrometer (Strapp et al., 1992), with an uncertainty of 34%. There were several instruments measuring various NO_y species: a six-channel cavity ring-down spectroscopy (CRDS) instrument from NOAA measured NO , NO_2 , O_3 (stated uncertainty of 4% (Fuchs et al., 2009; Wagner et al., 2011; Washenfelder et al., 2011; Wild et al., 2014)), NO_y via thermal dissociation-CRDS (stated uncertainty 12% (Wild et al., 2014)), and N_2O_5 (stated uncertainty 12% (Dubé et al., 2006; Fuchs et al., 2008; Wagner et al., 2011)). NO_3 from this instrument was not reported for WINTER due to low mixing ratios and uncertainties in inlet transmission efficiency for this species (Brown et al., 2016, 2017) with the configuration used on the C-130. A thermal dissociation laser-induced fluorescence (TD LIF) instrument from University of California Berkeley measured NO_2 with a stated uncertainty of 10% and HNO_3 with 25% uncertainty (Day et al., 2002). Measurements of peroxy and alkyl nitrates, also by the TD LIF, were influenced by large mixing ratios of other wintertime nitrogen species (ClNO_2 , N_2O_5) and are not used in this analysis. A chemiluminescence detector from the National Center for Atmospheric Research (NCAR) measured NO , O_3 , and NO_y (uncertainties 10, 5 and 20%, respectively) (Ridley et al., 1994) but was unavailable on the Atlanta flight. An I^- CIMS from University of Washington measured HNO_3 , N_2O_5 , and ClNO_2 with stated uncertainties of 15% (Kercher et al., 2009; Lee et al., 2014). In addition, a pulsed UV fluorescence instrument from NOAA measured SO_2 (Ryerson et al., 1998), and a laser-induced fluorescence instrument measured formaldehyde (Cazorla et al., 2015). The trace organic gas analyzer (Apel et al., 2015) on the airplane was not available for this flight, but acetaldehyde (uncertainty of 20%) data from other flights were scaled with formaldehyde (Figure S1 in the supporting information; further discussion below). Performance characteristics are given in the individual references listed above, and intercomparison papers between different reactive nitrogen instruments are currently in preparation. Instruments for NO_2 (CRDS and LIF), NO_y and O_3 (CRDS and chemiluminescence) agreed to within stated uncertainties. Agreement between the CRDS and chemiluminescence NO instruments was within 25% for eight of nine flights with concurrent data, and 38% on an additional flight, with a high bias (average 21%) for CRDS. Agreement between CRDS and CIMS N_2O_5 was within 40% for 10 research flights with nighttime data and within 5% on average.

2.2. Dispersion Modeling

Dispersion modeling was done using a two-dimensional box model of horizontal mixing and nitrogen oxide chemistry, adapted from the model used by Brown et al. (2012). The model was initialized with a plume containing only NO (i.e., no direct NO_2 emission (Peischl et al., 2010)) and a width of 0.1 km (the width of a single grid box in the model.) The background was set to contain O_3 and representative organic compounds that drive organic nitrate formation through reaction with NO_3 (see reaction scheme below). Background O_3 values were varied at 30, 40, and 50 ppbv. The 30 and 40 ppbv constrain the observed backgrounds in different portions outside the plume, while 50 ppbv was included to investigate the effect of a higher O_3 background, characteristic of other regions of the U.S. (Brown et al., 2013), and potentially increasing wintertime O_3 in the southern U.S. (Bloomer et al., 2010). Propene, acetaldehyde, and monoterpenes were the organic compounds included to represent NO_3 reactions. Although not a comprehensive list, these three compounds were chosen to represent reactivity with anthropogenic, oxygenated, and biogenic VOCs, respectively. Fast response gas chromatography-mass spectrometry VOC measurements were part of the WINTER payload but were unavailable on this flight, so background organic concentrations were taken from literature data for the southeast U.S. Isoprene was not included in this analysis, as wintertime concentrations should be close to 0 (Hagerman et al., 1997). Monoterpene concentrations of 0.05 to 0.5 ppbv were used as lower and upper limits to bracket wintertime concentrations observed in the greater Atlanta area based on previous, surface level measurements in the southeast U.S. (Hagerman et al., 1997). Alkenes were

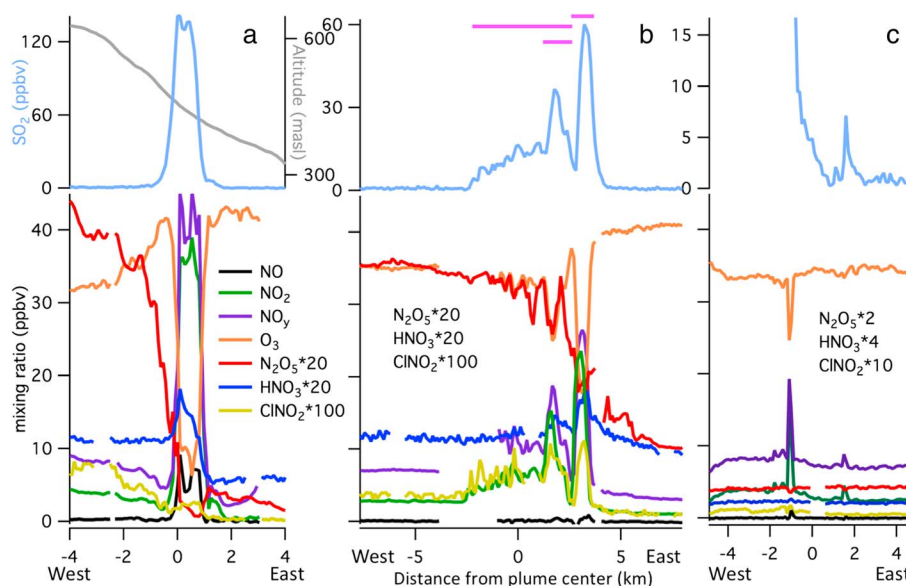


Figure 1. The mixing ratios of SO_2 and NO_y species in three plume intercepts at two downwind distances from the Harlee Branch Power Plant. Intercept (a) was 5 km from the plant, while (b) and (c) were 40 km from the plant and two different altitudes. The closer-in intercept was taken while ascending, so it covers 80 m of vertical depth over the 1.5 km of horizontal that contained the plume. Of the farther out intercepts, (b) was taken at 472 m agl and (c) at 621 m agl. The pink bars on (b) indicate the portions of the plume width used to determine effective dispersion of the plume. In all intercepts, NO_y , NO , and N_2O_5 shown are from the CRDS instrument. In intercept (b), the NO_2 measurement is from the TD LIF, as the CRDS was zeroing during the plume. ClNO_2 and HNO_3 in all plumes were from the I^- CIMS.

represented by propene and a range of 0.2 to 1.0 ppbv was used, spanning the wintertime range measured by Hagerman et al. (1997) in Yorkville, GA. Data from 1997 may represent an upper limit for alkene concentrations in 2015, as analyses of urban VOC emissions trends from Los Angeles, CA, have shown steep declines in nearly every VOC class (Warneke et al., 2012). In other studies in the eastern U.S., however, propene, specifically, has shown no discernable interannual trends from 2004 through 2010 (Russo et al., 2010), so 0.5 ppbv is a reasonable upper limit. Acetaldehyde was measured on other flights in the series and showed a reasonably strong relationship with formaldehyde (Figure S1). Therefore, a relationship of acetaldehyde in pptv equal to $0.82 * \text{HCHO} + 160$ was used to calculate acetaldehyde concentrations on this flight. The range of 0.5 to 1 ppbv was used to represent the span of values calculated.

NO in the plume model was initialized at 40, 59, and 100 ppbv to represent that ambient concentration immediately after mixing of the plume with ambient air into the smallest horizontal plume grid cell. The 40 ppbv value is approximately equal to the peak value measured in the closest plume intercept (Figure 1a). The 59 and 100 ppbv values are based on Continuous Emissions Monitoring System (CEMS) data (<https://ampd.epa.gov/ampd/>) showing that historical NO_x emissions were 1.5 times higher from 2003 to 2008 and 2.5 times higher than 2015 from 1995 to 2002. The change in 2002 is due to implementation of a low NO_x cell burner. There is no indication in the CEMS inventory of what induced the change in 2008. All mixing ratio values used are somewhat arbitrary and not intended to reproduce emissions inventories in an absolute comparison. The higher values are therefore calculated in relative ratios to the observed mixing ratio of 40 ppbv.

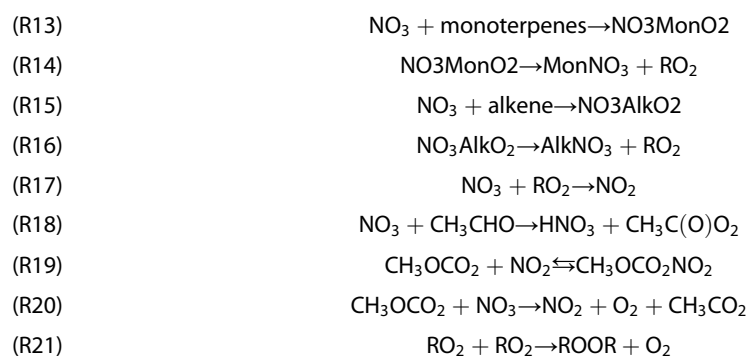
The total first-order N_2O_5 loss rate coefficient ((R4) and (R5)) was varied over three values, 5.31×10^{-6} , 1.80×10^{-5} , and $1.10 \times 10^{-4} \text{ s}^{-1}$. The lowest value is derived from the net increase of HNO_3 and ClNO_2 observed between the plant emissions and downwind intercept, based on the wind speed and assuming no depositional loss. Assumption of a constant wind speed, as measured on the C-130, between intercepts results in a transport time estimate of 5.8 h, yielding a very low loss rate constant. The middle value uses the time from a Hybrid Single-Particle Lagrangian Integrated Trajectory (HYSPPLIT) back trajectory, which shows 3.0 h of transport time between the plant and the downwind intercept. The N_2O_5 loss rate coefficient of $1.1 \times 10^{-4} \text{ s}^{-1}$ is the value used in Brown et al. (2012) for a similar analysis. This value was included to allow more direct comparison with previous results and to provide contrast to the anomalously low N_2O_5 uptake and aerosol surface area during this flight. The aerosol surface area, corrected for relative humidity, varied between 100 and

Table 1
 Parameters Used in Box Model

Parameter	A	B	C
Mixing rate (m ² /s)	0.8	2	30
N ₂ O ₅ loss rate (s ⁻¹)	5.3 × 10 ⁻⁶	1.8 × 10 ⁻⁵	1.1 × 10 ⁻⁴
Initial NO (ppbv)	40	59	100
O ₃ background (ppbv)	30	40	50
Monoterpenes/alkenes/ aldehydes (ppbv)	0.05/0.2/0.5	0.5/1/1	
ClNO ₂ yield	0	1	

200 μm²/cm³, with no enhancement above the variation of one standard deviation, 14 μm²/cm³, in the power plant plumes. Background near the plume was 114 μm²/cm³, so that value was used to calculate N₂O₅ uptake from the N₂O₅ loss rate coefficient. The aerosol composition within the plume showed no variation from background composition, including a lack of sulfate or nitrate enhancement. The rate of oxidation of sulfur is slow in the absence of OH sources, so as long as the source does not directly emit sulfate aerosol or a sulfate precursor more reactive than SO₂ (e.g., SO₃), little sulfate oxidation is expected at night (Brown et al., 2007). The lack of NO₃⁻ enhancement is consistent with the low N₂O₅ loss rate coefficient.

ClNO₂ yields (Φ) of 0 and 1 were used to bracket partitioning of N₂O₅ loss between solely HNO₃ (R4) and ClNO₂ + HNO₃ (R5). The following reaction scheme was included in the plume model in addition to (R1)–(R5).



Here MonNO₃ and AlkNO₃ indicate nitrates formed from reactions of NO₃ with monoterpenes and anthropogenic alkenes, respectively. For simplicity, nitrate yields from these reactions are assumed to be unity and serve as an upper limit for organic NO₃⁻ production. The assumption of unit yield of organic nitrates in the reaction of NO₃ with organic compounds potentially overestimates the production of these compounds. Nonunit organic nitrate yields lead to regeneration of NO_x as NO₂ (Hallquist et al., 1999). To the extent that reactions of NO₃ with BVOC are a significant loss for NO₃ within plumes at night, the analysis will overestimate the rate of NO_x loss. Such effects are more likely to be important in the summer, when BVOC emissions are high (Edwards et al., 2017), than in the winter plumes modeled here.

All RO₂ are assumed equivalent with a single RO₂ + HO₂ rate coefficient for (R17) equivalent to NO₃ + HO₂ and for (R20) an average of HO₂ + HO₂, HO₂ + CH₃O₂, and CH₃O₂ + CH₃O₂. International Union of Pure and Applied Chemistry recommendations were used for all reaction rate constants (Atkinson et al., 2004; Atkinson et al., 2006). For the monoterpene reaction, the value for NO₃ + α-pinene was used both because α-pinene is the most abundant of the monoterpenes, and the reaction rate is intermediate between that of the fastest (limonene) and slowest (β-pinene) reacting species. For the anthropogenic alkene reaction, the propene rate constant was used as propene is much faster reacting than ethene (~5×) but much greater in abundance than higher alkenes and thus should have the greatest effect on NO₃ reactivity of the alkenes (Brown et al., 2011).

At each time step, the horizontal dispersion constant ($k = 0.8, 2$ or $30 \text{ m}^2 \text{ s}^{-1}$, see derivation of these values in results) was applied across the plume width, horizontally mixing the concentrated emissions with the background O₃ and organic compounds. The horizontal dispersion constant describes mixing that is proportional to a concentration gradient, formally equivalent to a molecular diffusion constant even though the dispersion is based on empirical observation of downwind plume widths and is much more rapid than molecular diffusion. Numerical integration to calculate the concentration, C_i , of a species in the i th box follows equation (1).

$$\frac{dC_i}{dt} = \frac{k}{\Delta x^2} (\Delta C_i^L + \Delta C_i^R) + \frac{\partial C_i^{\text{Chem}}}{\partial t} \quad (1)$$

Here k is a constant, representing the horizontal dispersion, with units of length² time⁻¹; Δx is the length of the horizontal box used in the integration; ΔC_i^L and ΔC_i^R are the concentration differences between the i th

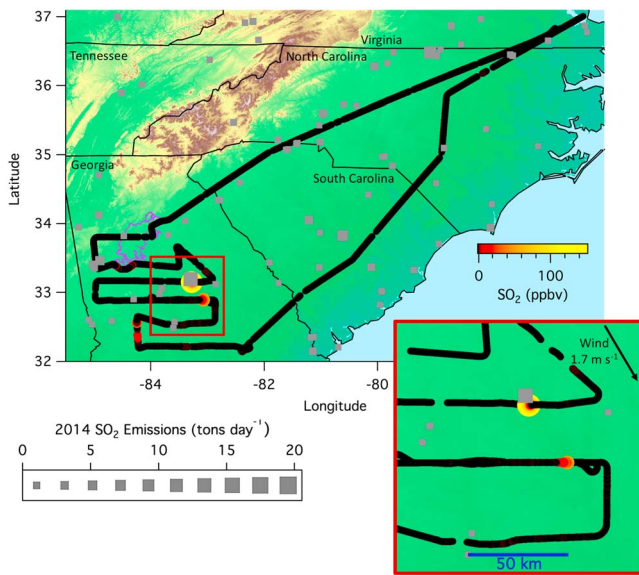


Figure 2. Flight path for research flight on 7 March 2015. Flight track is colored and sized by SO₂ mixing ratio. The grey squares are power plants, sized by annual SO₂ emissions. The Atlanta metro area is outlined in purple. The inset is where the plume from Harlee Branch was encountered. The path farther from the plant has two plume intercepts directly on top of one another.

in shape when plotted against the horizontal transect, as a simple plume dispersion model would predict, it was taken while changing altitude and, therefore, a part of the observed width may have been due to the variation of the plume in the vertical dimension. Several species had significantly different backgrounds on the upper and lower sides of the plume. O₃ was not fully reacted away in the plume center, but NO was still present, indicating that the plume intercept was close enough to the plant that conversion of NO to NO₂ via (R1) had not gone fully to completion.

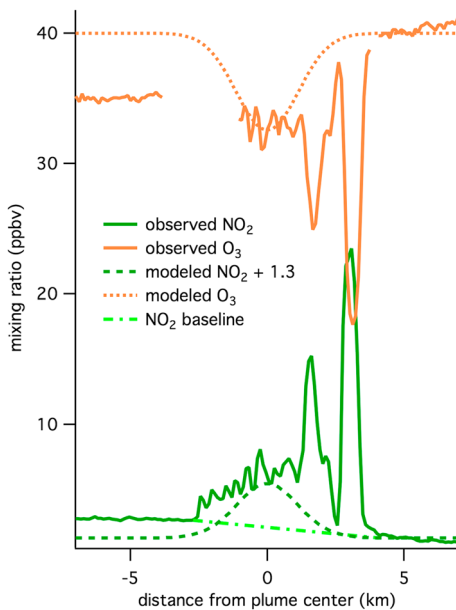


Figure 3. Comparison of observed and modeled NO₂ and O₃. The model results are taken at 5.8 h from the initial conditions. The run includes a mixing rate of 30 m²/s, a N₂O₅ loss rate coefficient of 5.6 × 10⁻⁶, initial NO mixing ratio of 59 ppbv, initial O₃ mixing ratio of 40 ppbv, low organic concentration, and Φ_{CINO2} of 1. The modeled NO₂ is offset by 1.3 to better compare to the observations. The lighter green dotted line is the interpolated baseline that was subtracted from the NO₂ observations to produce peak areas.

box and the adjacent box to the left or right; and $\frac{\partial C_{Chem}}{\partial t}$ is the concentration change due to chemistry during the time step.

All parameters determined above were run symmetrically in the box model (Table 1). That is, every combination of all parameters was run, giving a total of 324 unique model scenarios.

Nighttime horizontal plume transects were either non-Gaussian or made up of a series of Gaussian plumes of different widths and heights. Application of a horizontal Gaussian plume dispersion model therefore does not represent their evolution quantitatively, although the use of a variety of dispersion constants does capture the range in variability that can be attributed to different dispersion rates.

3. Results

Multiple passes were made of the plume from the Harlee Branch power plant on 7 March 2015 (Figure 2). The plant, located in Putnam County, GA, has since been closed, but the observations of the plume can inform our understanding of plume behavior from other plants. Throughout the flight, the ambient temperature was 4°C with very little variation.

While the first pass, 5.6 km from the plant and 19 min downwind, based on onboard wind speed measurement, was close to Gaussian in shape when plotted against the horizontal transect, as a simple plume dispersion model would predict, it was taken while changing altitude and, therefore, a part of the observed width may have been due to the variation of the plume in the vertical dimension. Several species had significantly different backgrounds on the upper and lower sides of the plume. O₃ was not fully reacted away in the plume center, but NO was still present, indicating that the plume intercept was close enough to the plant that conversion of NO to NO₂ via (R1) had not gone fully to completion. Odd oxygen (O_x = O₃ + NO₂) was approximately conserved in the near-field intercept, increasing by about 5% within the plume, compared with the regions immediately outside of it. This increase is consistent with direct emissions of NO₂ from power plants (Peischl et al., 2010). The O₃ and NO concentrations were nearly equal at the plume center, so the degree of downwind O₃ removal at plume center will depend critically on the rate of mixing compared to the reaction rate of (R1).

The downwind transects of the plume indicate some vertical mixing of the plume and varied amounts of horizontal mixing, depending on how they are interpreted (Figure 1). The plume width can also vary, dependent on where, vertically within the plume, the plume is transected. There are two passes of the plume, 39 km downwind from the plant. The transects are at 603 and 752 m above sea level (asl) (472 and 621 m above ground level (agl)), one directly on top of the other, putting a lower bound on plume depth of 149 m. Both plume intercepts show agreement between the NO_y measurement and the sum of measured NO_y species (NO + NO₂ + 2*N₂O₅ + ClNO₂ + HNO₃). Other forms of NO_y, such as peroxyacetyl nitrates or organic nitrates, are expected to be small in these nighttime plume intercepts. In the lower intercept, the sum of NO_y versus the measured NO_y has a slope of 1.05 and R² of 0.99. Here NO₂ (NO_y - NO_x) is 12% of the NO_y, so the agreement is well within the measurement errors noted in section 2.1. In the higher-altitude intercept, the slope is 1.09 and R² is 0.99. Both

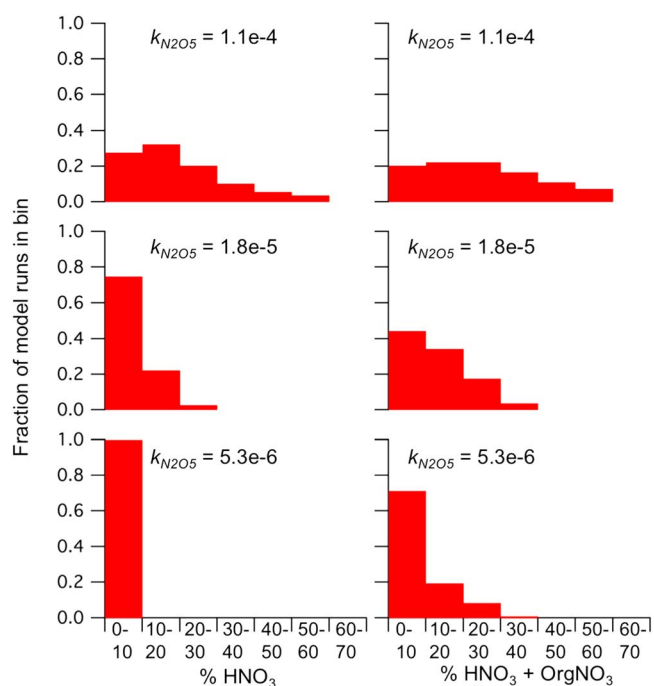


Figure 4. Distribution from all 324 model simulations of percent of NO_x converted to HNO_3 and HNO_3 and organic nitrates at 12 h downwind of the plant with three N_2O_5 loss rate constants ($k_{\text{N}_2\text{O}_5}$). The organic nitrates represent an upper limit based on the assumption of unit yield from $\text{NO}_x + \text{VOC}$ reactions (see text). The lowest $k_{\text{N}_2\text{O}_5}$ ($5.3 \times 10^{-6} \text{ s}^{-1}$) value is calculated from the amount of HNO_3 formed in the downwind plume intercept and a transit time of 5.8 h, based on wind speed. The $1.8 \times 10^{-5} \text{ s}^{-1}$ was calculated the same way, but with a transit time of 3.0 h, derived from HYSPLIT. The highest $k_{\text{N}_2\text{O}_5}$ is from Brown et al. (2012) and included for comparison with other studies.

slopes are unity to within the combined measurement uncertainties of the reported species. For further analysis, NO , NO_y , and N_2O_5 measurement were used from the CRDS and HNO_3 and ClNO_2 measurements were from the I^- CIMS instrument. NO_2 in the first intercept was from the CRDS, while in the second (at 603 m asl) was from the TD LIF, as the CRDS was zeroing during that intercept. During the first intercept, the CRDS versus TD LIF NO_2 measurements show a slope of 1.04 and R^2 of 0.97, while throughout the entire flight the slope is 0.99 and R^2 0.98, so the choice between instruments should not affect this analysis.

The upper intercept has much lower concentrations and seems to be near the vertical apex of the plume extent. The downwind plumes also have significantly different background concentrations on the two sides of the plume due to the presence of the Atlanta urban plume on the west side of the Harlee Branch power plant plume. In these transects, NO was no longer present and the minimum O_3 was 18 ppbv, indicating that even if O_3 was completely reacted away during a portion of the transport between the two intercept distances, mixing incorporated excess O_3 . Modeling dispersion to match the plume as observed is difficult, as it is not Gaussian. We can, however, match various peak widths, modeled as Gaussian fits. The non-Gaussian nature of the plume, however, indicates other mixing processes in play, beyond simple horizontal dispersion. This raises the question of which portion(s) of the plume should be assumed to be exclusively the result of dispersion of the plume. A model of just the easternmost part of the plume, the portion with the highest concentrations of all species and the most Gaussian shape, gives a dispersion constant of $0.8 \text{ m}^2 \text{ s}^{-1}$ starting from a plume of 0.1 km, 5.8 h away. The same dispersion constant does not match the plume observed 19 min from the source, but the difference could be due to transects of different vertical portions of the plume or from variations of the dispersion with time. If the middle portion of the plume is modeled, a dispersion constant

of $2 \text{ m}^2 \text{ s}^{-1}$ is required, and to model the entire western portion of the plume, $30 \text{ m}^2 \text{ s}^{-1}$ is needed (Figure 1). These dispersion constants encompass the value of $5 \text{ m}^2 \text{ s}^{-1}$ used by Brown et al. (2012) to model nighttime horizontal dispersion of power plant plumes in Texas.

The chemical evolution of the plume is highly dependent on the value for N_2O_5 uptake ($\gamma_{\text{N}_2\text{O}_5}$) and aerosol surface area (S_A). Together, these values give the first-order N_2O_5 loss rate coefficient, $k_{\text{N}_2\text{O}_5}$, according to equation (2).

$$k_{\text{N}_2\text{O}_5} = \frac{1}{4} * \bar{c} * S_A * \gamma_{\text{N}_2\text{O}_5} \tag{2}$$

Using wind speed and direction as observed in the plume, and applying a simple iterative box model to fit enhanced N_2O_5 present in the downwind plume intercept (with linearly interpolated background N_2O_5 subtracted out), both $\gamma_{\text{N}_2\text{O}_5}$ and the $k_{\text{N}_2\text{O}_5}$ loss rate constant are small, with $\gamma_{\text{N}_2\text{O}_5} = 6.97 \times 10^{-4}$ and $k_{\text{N}_2\text{O}_5} = 5.3 \times 10^{-6} \text{ s}^{-1}$ (equivalent to an N_2O_5 lifetime >50 h), respectively. With $k_{\text{N}_2\text{O}_5} = 5.3 \times 10^{-6} \text{ s}^{-1}$ and a traveltime of 5.8 h, the model and observations match well in NO_x conversion (Figure 3). With starting conditions of 40 ppbv NO , 30 ppbv background O_3 , an effective dispersion constant of 0.8, and a ClNO_2 yield of 1, the model shows much less than 1% conversion of NO_x to HNO_3 and the only significant NO_z contribution from N_2O_5 .

Current parameterizations of $\gamma_{\text{N}_2\text{O}_5}$ (Bertram & Thornton, 2009; Davis et al., 2008; Evans & Jacob, 2005; Gaston et al., 2014) do not reproduce such low values. In comparison, Brown et al. (2012) used $k_{\text{N}_2\text{O}_5} = 1.1 \times 10^{-4} \text{ s}^{-1}$ in summertime power plant plumes in the Houston area based on the average of prior determinations of uptake coefficients from that region that had an average value of 3×10^{-3} (Brown et al., 2009). Low relative humidity (50–55%) in the region area on this flight may be partially responsible for low $\gamma_{\text{N}_2\text{O}_5}$ values. It is also

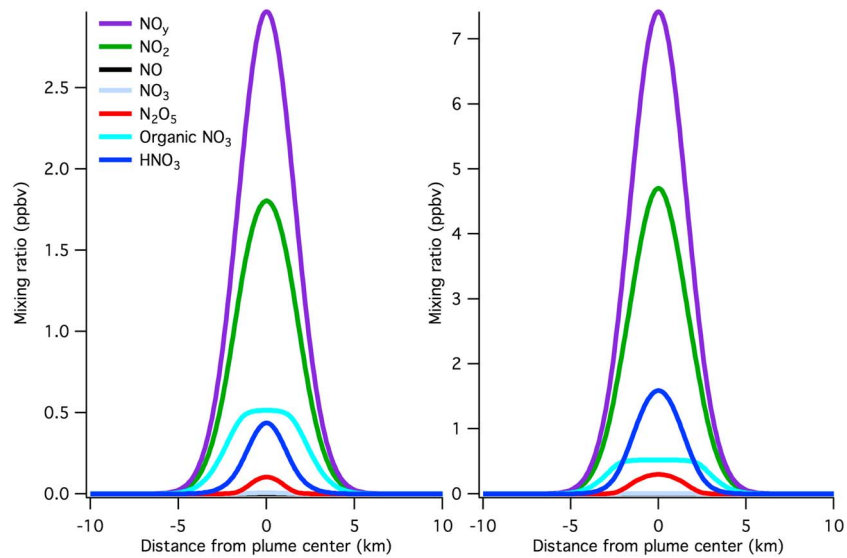


Figure 5. Transects of modeled plumes at 12 h downwind from the model run with $k_{\text{N}_2\text{O}_5}$ of $1.1 \times 10^{-4} \text{ s}^{-1}$, high organic backgrounds, mixing rate of $30 \text{ m}^2 \text{ s}^{-1}$, O_3 background of 30 ppbv, ClNO_2 yield of 0, and initial NO of (left) 40 ppbv and (right) 100 ppbv. There is greater relative HNO_3 production in the plume with higher initial NO_x , but lower production of organic nitrates.

possible that the organic content of the aerosols acted to suppress N_2O_5 uptake as has been observed in previous laboratory studies, though those studies generally show extremely high organic fractions required to suppress $\gamma_{\text{N}_2\text{O}_5}$ to this degree (Anttila et al., 2006). In the plumes, the organic content of the aerosol was 35–40% of the aerosol mass (as determined by aerosol mass spectrometer). Anttila et al. (2006)

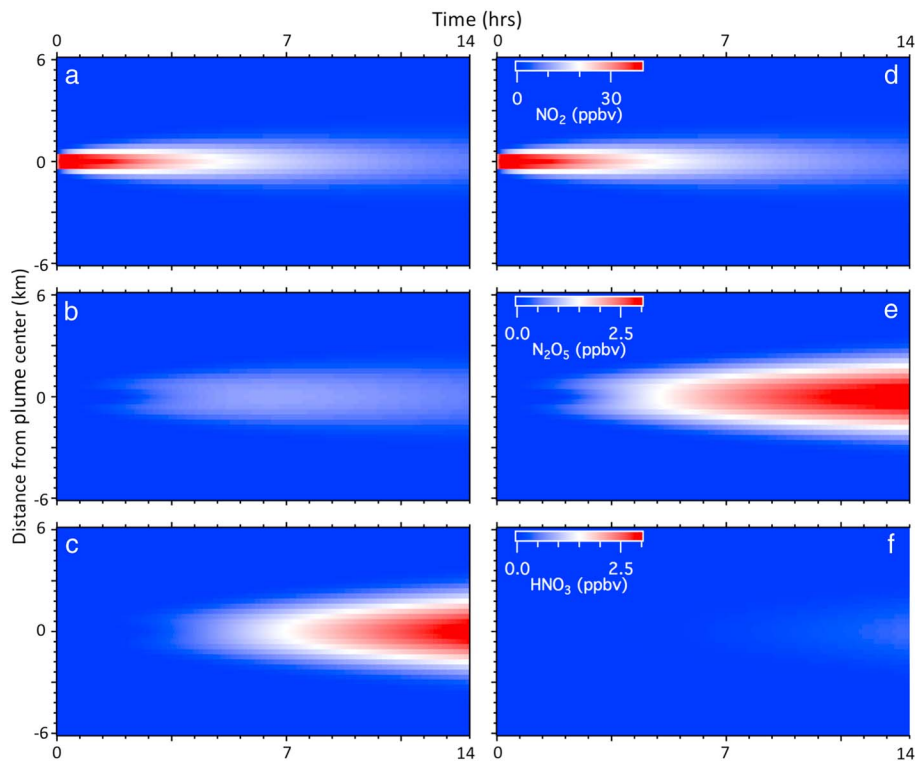


Figure 6. The evolution of the modeled plume for two different $k_{\text{N}_2\text{O}_5}$ values. All panels have a dispersion rate of $2 \text{ m}^2 \text{ s}^{-1}$, initial NO of 59 ppbv, background O_3 of 40 ppbv, low background organic mixing ratios, and ClNO_2 yield of 0. On the left are (a) NO_2 , (b) N_2O_5 , and (c) HNO_3 for $k_{\text{N}_2\text{O}_5}$ of $1.1 \times 10^{-4} \text{ s}^{-1}$, while on the right (d) NO_2 , (e) N_2O_5 , and (f) HNO_3 , all have $k_{\text{N}_2\text{O}_5}$ of $5.3 \times 10^{-6} \text{ s}^{-1}$. Both the left and right plots use the same mixing ratio color scale.

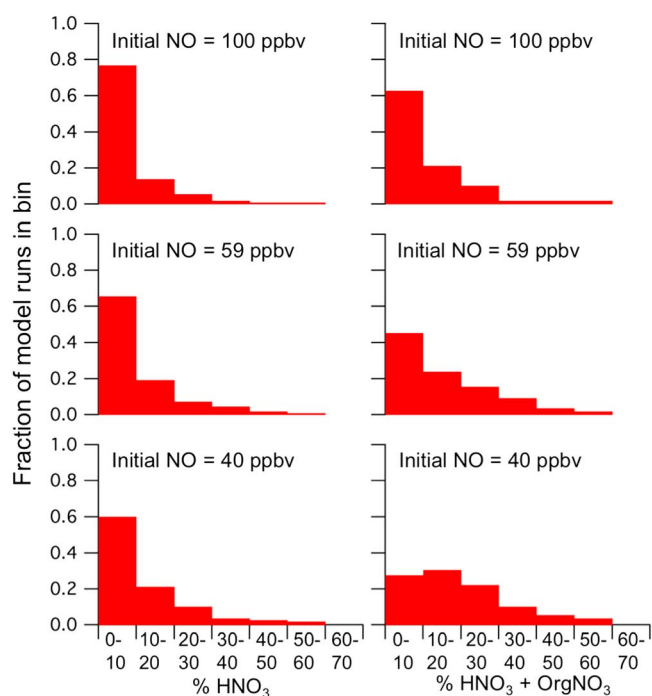


Figure 7. Distribution of percent of NO_y converted to HNO₃ and HNO₃ + organic nitrates (upper limit as in Figure 4) in all 324 model simulations at 12 h downwind of the plant with three initial NO concentrations. The 40 ppbv NO was determined by the NO_x mixing ratio in the intercept closest to the plant. The higher mixing ratios scale the observed initial mixing ratio to relative changes in historical emissions from the continuous emission monitoring system, which were 1.5 and 2.6 times higher with different NO_x emission controls.

minutes (Darer et al., 2011). These reactions, however, can be acid-catalyzed, and the rate of hydrolysis of primary nitrates can approach that of tertiary nitrates if the aerosol pH is less than 0 (Rindelaub et al., 2016). In the Atlanta area, the aerosol pH was frequently less than 0 and always less than 2 (Guo et al., 2016), so both primary and tertiary nitrates taken up on aerosol should be expected to hydrolyze quickly and result in HNO₃ formation, though the very low aerosol surface area may reduce HNO₃ formation from all organic nitrates. If the NO_x forms a terminal product overnight (via direct production of HNO₃ or through organic reactions), the next day it cannot participate in further O₃ chemistry, it will not be transported as far downwind, and it can control patterns of acid deposition downwind (Dentener & Crutzen, 1993).

All model simulations shown here were run at 4°C, the observed ambient temperature. If the temperature were higher, as in summer, all reactions will proceed faster and more HNO₃ and organic nitrates would be generated, all else remaining the same. We, however, expect many of the modeled factors, especially organic compound background mixing ratios, to also change with temperature, further altering the NO_x removal. The factors that control on how much NO_x is removed from a power plant plume at 4°C overnight that will be discussed individually in the sections below.

4.1. N₂O₅ Loss Rate Constant ($k_{N_2O_5}$)

The factor that independently exerts the most control over the range of conditions surveyed in this model is the N₂O₅ loss rate constant ($k_{N_2O_5}$). When $k_{N_2O_5}$ is very low, whether driven by low N₂O₅ uptake or low aerosol surface area, no other conditions can yield NO_x conversion to HNO₃ greater than 10% (Figure 4). The percent of HNO₃ is calculated as the integrated area for HNO₃ across the modeled plume transect (Figure 5) compared with the integrated area of NO_y across the transect, since model NO_y is conserved throughout the plume. As expected, the plume evolution shows that N₂O₅ persists and less HNO₃ is formed when $k_{N_2O_5}$ is lower (Figure 6). This is true throughout the plume, with little N₂O₅ buildup at the highest

found that a coating of greater than 200 nm was required on a 600 nm diameter particle (greater than 90% organic content required) to give a $\gamma_{N_2O_5}$ on the order of 10⁻⁴.

The yield of ClNO₂ (Φ) observed in the plume was 1 (all N₂O₅ followed (R5), none (R4)), based on the ratio of ClNO₂ to HNO₃ in the plume, with the linearly interpolated background values subtracted out. It is possible that this is influenced by direct emissions of halogen from the power plant (Riedel et al., 2013) or simply a result of the very low $\gamma_{N_2O_5}$ and therefore the small amount of Cl required for ClNO₂ production.

4. Discussion

NO_x can be removed from the atmosphere via two pathways. The first pathway, formation of HNO₃, is normally a terminal product of NO_y chemistry in the lower atmosphere (e.g., (R4) and (R10)). The second is formation of organic nitrates ((R13)–(R19)), but the degree to which these compounds represent a terminal NO_x sink depends on what fraction of organic nitrates are removed (via conversion to HNO₃, another terminal product, or deposition) or further processed back into NO_x via oxidation reactions or photolysis. Monoterpene nitrates dominate organic nitrate formation in this model (see further discussion, below); therefore, the branching between monoterpene nitrates that recycle back to NO_x via oxidation and those that form HNO₃ or another terminal NO_x product will be most important. Monoterpenes can form a mixture of primary and tertiary nitrates (Rindelaub et al., 2016). Laboratory studies have found that primary organic nitrates hydrolyze, resulting in HNO₃ formation, on a time-scale of months, while the tertiary nitrates hydrolyze on the order of

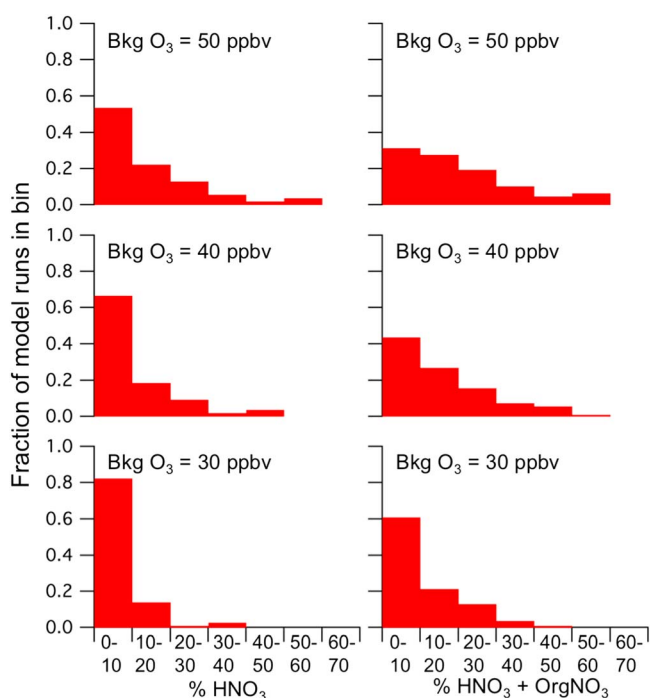


Figure 8. Model distribution for all 324 simulations of percent of NO_y converted to HNO₃ and HNO₃ + organic nitrates (upper limit) at 12 h downwind of plant with three O₃ backgrounds. The three backgrounds come from the range of O₃ observed on the 7 March research flight.

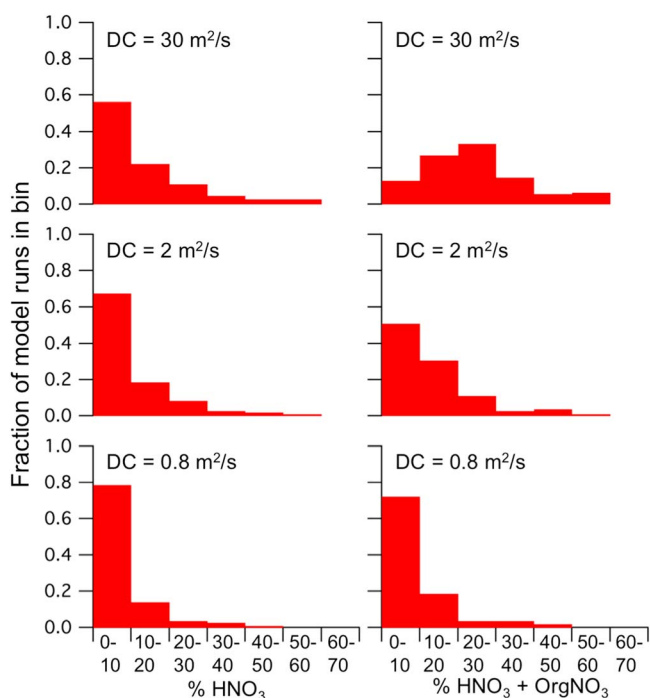


Figure 9. Distribution of percent of NO_y converted to HNO₃ and HNO₃ + organic nitrates in all 324 model simulations at 12 h downwind of the plant with three dispersion constants (DC). The mixing rates were calculated to match the width of different portions of the downwind intercept.

$k_{N_2O_5}$, which corresponds to greater HNO₃ concentrations. In contrast, at low $k_{N_2O_5}$ values, N₂O₅ builds up throughout the plume’s lifetime, while little HNO₃ is produced.

The N₂O₅ loss rate constant decreases in importance when including organic nitrates in the total NO_x removed. Even at the lowest $k_{N_2O_5}$ value, up to 31% of NO_x can be converted to HNO₃ and organic nitrates combined. At the lowest N₂O₅ loss rate, the highest fraction of NO_x removal (production of HNO₃ + organic nitrates) occurs when VOC concentrations are high and the initial NO_x mixing ratio is low.

The lowest calculated N₂O₅ loss rate constant, $5.3 \times 10^{-6} \text{ s}^{-1}$, is somewhat lower than what has been previously reported in the literature. This is driven in part by the moderately low observed aerosol surface area of $120 \mu\text{m}^2/\text{cm}^3$, but still requires a low $\gamma_{N_2O_5}$ of 7.0×10^{-4} . This is slightly lower than the low end ($\gamma_{N_2O_5} = 1 \times 10^{-3}$) of reported values from analysis of field data (Brown & Stutz, 2012), but within the range of reported laboratory values. A laboratory study of pure organic and organic coated aerosols found $\gamma_{N_2O_5}$ of $4.5\text{--}5.9 \times 10^{-4}$ (Anttila et al., 2006). The middle loss rate constant, $1.8 \times 10^{-5} \text{ s}^{-1}$, has a corresponding uptake coefficient, $\gamma_{N_2O_5} = 2.37 \times 10^{-3}$, which falls on the low end of the range of previously reported values from field studies. As in prior analysis of aircraft data (Brown et al., 2009), the reason for these low $\gamma_{N_2O_5}$ values is not clear and remains an active area of study.

The low N₂O₅ uptake observed in the plume is broadly consistent with high levels of observed N₂O₅, and thus low N₂O₅ reactivity, within the Atlanta plume during the same research flight, so it is not likely a consequence of chemistry specific to this particular power plant plume. Steady state lifetimes of N₂O₅, derived from the steady state approximation (Brown et al., 2003), ranged between 9 and 14 h (equivalent to $k_{N_2O_5} = 2\text{--}3 \times 10^{-5} \text{ s}^{-1}$) (Figure S2). The low $k_{N_2O_5}$ values were, again, partially driven by low aerosol surface area ($72 \mu\text{m}^2/\text{cm}^3$), and the corresponding $\gamma_{N_2O_5}$ values were $4\text{--}6 \times 10^{-3}$. Whether the low uptake is more typical of wintertime chemistry in this area or particular to the conditions of this flight is not currently known, though Wagner et al. (Wagner et al., 2013) found mostly higher values of $\gamma_{N_2O_5}$, 0.002–0.04, in wintertime at a ground site in Colorado near power plant emissions.

4.2. Initial NO and O₃ Background

While prior studies have demonstrated that reductions in NO_x emissions stemming from recently implemented NO_x control technology are a primary controlling factor in the amount of NO_x removed by nighttime chemistry (Brown et al., 2012), the degree to which this is true depends on a variety of other factors, including those listed above. Brown et al. (2012) showed that as NO emissions were decreased for two power plant plumes sampled in Texas in October 2006, the percentage of NO_x converted to HNO₃ increased, as plumes no longer had all O₃ reacted away, and chemistry could progress to (R2) and beyond. Figure 7 shows that this effect is generally true for the conditions modeled here, in that smaller fractions of NO_x to HNO₃ or HNO₃ + organic nitrates occur for increasing initial NO in the simulations, consistent with generally slower nighttime chemistry at decreased plume O₃ mixing ratio. There are, however, some

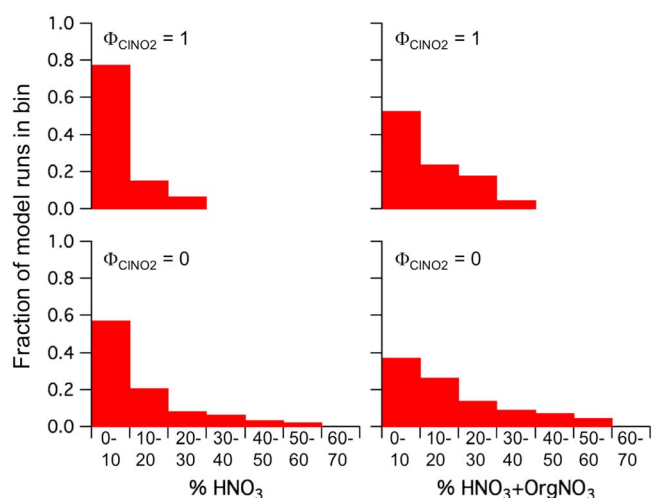


Figure 10. Distribution of percent of NO_y converted to HNO_3 and HNO_3 + organic nitrates at 12 h downwind for all model simulations of the plant with two ClNO_2 yields (Φ). While the observed ClNO_2 yield in the plume is close to 1 (0.96), we can capture the full range of potential ClNO_2 yields between 0 and 1.

conditions under which a larger percentage of NO_x is converted to HNO_3 when the initial NO is higher. This happens when both the mixing rate and background VOC concentrations are high. This is due to competition with HNO_3 and organic nitrate formation, where at higher background VOC levels, (R12)–(R13) and (R14)–(R15) are favored over (R3)–(R5). Under those conditions, the percent of NO converted to HNO_3 and organic nitrate decreases with increasing NO_x emissions. For instance, with an N_2O_5 loss rate constant of $1.1 \times 10^{-4} \text{ s}^{-1}$, mixing rate of $30 \text{ m}^2 \text{ s}^{-1}$, O_3 background of 30 ppbv, ClNO_2 yield of 0, and a high monoterpene background of 0.5 ppbv, the percent of NO_x converted to HNO_3 increases from 10.4 to 17.7 as the initial NO increases from 40 to 100 ppbv. Over the same conditions, the HNO_3 and organic nitrates combined decrease from 33 to 29% (Figure 5 and Table S1).

The effect of NO emissions on NO_x removal is also intimately tied to the background O_3 level. When background O_3 is higher, complete O_3 removal, due to (R1), is less likely. In fact, the only model conditions under which NO is still present after 12 h involve the smallest mixing rate, initial NO of 100 ppbv and O_3 background levels of 30 or 40 ppbv.

The 30 ppbv O_3 background leaves NO as 15% of NO_y after 12 h, while the 40 ppbv background leaves 3% as NO . Under no other conditions is NO even 1% of NO_y after 12 h. If a small portion of NO_x emitted is NO_2 , rather than NO (Peischl et al., 2010), the NO to NO_2 step (R1) would go to completion faster, and the plume would have a slight excess of odd oxygen ($\text{O}_x = \text{O}_3 + \text{NO}_2$) early in its overnight evolution (Brown et al., 2006). The potential 2% difference in O_x is much smaller than other variations observed and modeled. Overall, within the range of conditions used, O_3 background has a larger influence on NO_x than the initial NO mixing ratio. At the lowest O_3 background, 30 ppbv, no other conditions result in HNO_3 greater than 40% of NO_y after 12 h (Figure 8). In contrast, even with an initial NO mixing ratio of 100 ppbv, it is possible to convert over 50% to HNO_3 after 12 h (Figure 7). While summertime O_3 levels are decreasing throughout the eastern U.S., wintertime levels are increasing (Bloomer et al., 2010), which will result in greater NO_x removal from plumes with decreased NO_x emissions from power plants.

The 30 ppbv O_3 background leaves NO as 15% of NO_y after 12 h, while the 40 ppbv background leaves 3% as NO . Under no other conditions is NO even 1% of NO_y after 12 h. If a small portion of NO_x emitted is NO_2 , rather than NO (Peischl et al., 2010), the NO to NO_2 step (R1) would go to completion faster, and the plume would have a slight excess of odd oxygen ($\text{O}_x = \text{O}_3 + \text{NO}_2$) early in its overnight evolution (Brown et al., 2006). The potential 2% difference in O_x is much smaller than other variations observed and modeled. Overall, within the range of conditions used, O_3 background has a larger influence on NO_x than the initial NO mixing ratio. At the lowest O_3 background, 30 ppbv, no other conditions result in HNO_3 greater than 40% of NO_y after 12 h (Figure 8). In contrast, even with an initial NO mixing ratio of 100 ppbv, it is possible to convert over 50% to HNO_3 after 12 h (Figure 7). While summertime O_3 levels are decreasing throughout the eastern U.S., wintertime levels are increasing (Bloomer et al., 2010), which will result in greater NO_x removal from plumes with decreased NO_x emissions from power plants.

4.3. Horizontal Mixing

The rate at which the plume mixes with background air also exerts significant control over NO_x removal (Figure 9). Higher mixing rates result in more O_3 entrainment in the plume and increase the rates of (R1) and (R2), resulting in greater conversion to HNO_3 and organic nitrates. With the highest dispersion constant ($30 \text{ m}^2 \text{ s}^{-1}$), there are no scenarios in which the plume still has complete O_3 removal after 12 h (Table S1).

4.4. ClNO_2 Yield

The yield of ClNO_2 (Φ) depends on competition between reactions (R4) and (R5) that together give a net reaction, (R22) where H_2O and HCl are present in the aerosol phase.



This direct competition between reactions means that when Φ is higher, less HNO_3 is produced and less NO_x is removed overnight. The degree of influence of Φ in HNO_3 formation is highly dependent on the other conditions in the plume and background air. The percent of NO_y as ClNO_2 after 12 h when the yield is unity ranges from 0.05% to 28%. When the $k_{\text{N}_2\text{O}_5}$ is $1.1 \times 10^{-4} \text{ s}^{-1}$, the mixing rate $3 \text{ m}^2 \text{ s}^{-1}$, the initial NO mixing ratio 59 ppbv, the O_3 background 50 ppbv, and the organic backgrounds low, 28% of

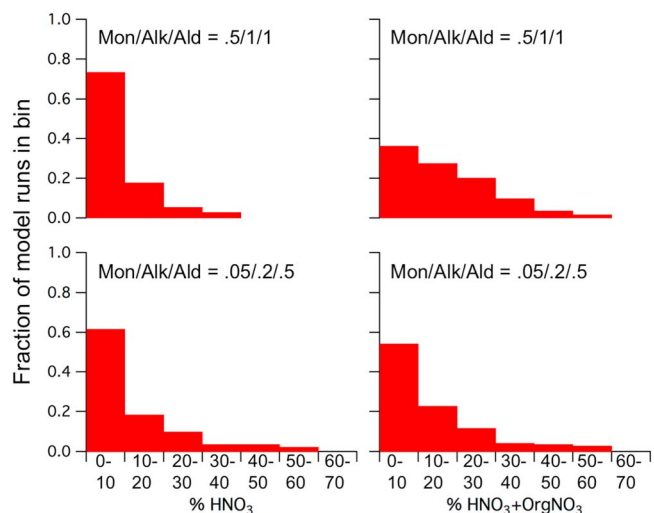


Figure 11. Model distribution for all simulations of percent of NO_y converted to HNO_3 and HNO_3 + organic nitrates at 12 h downwind of the plant with two levels of background VOCs. The ranges of monoterpenes (0.05–0.5 ppbv) and alkenes (0.2–1 ppbv) were from observation in Yorkville, GA (Hagerman et al., 1997). The range of acetaldehyde (0.5–1 ppbv) is calculated from the ratio of acetaldehyde to formaldehyde on other flights during WINTER and the formaldehyde measurements on this flight.

NO_y is ClNO_2 and another 28% is HNO_3 after 12 h with a ClNO_2 yield of 1. Overall, at a ClNO_2 yield of 0, more conditions allow for formation of higher levels of HNO_3 (Figure 10), though this condition may be unrealistic in power plant plumes. Riedel et al. (2013) found that in a power plant plume measured from a tall tower in Colorado, Φ ranged from 0.3 to 1, significantly higher than the background yields. Ambient conditions influencing Φ include the amount of aerosol nitrate and chloride, relative humidity, and aerosol hygroscopicity, which in turn may be driven by sulfate (Bertram & Thornton, 2009; Guo et al., 2016; Roberts et al., 2008; Roberts et al., 2009).

4.5. Background VOC Concentrations

The influence of background VOC concentrations has the least straightforward effect on NO_x removal in the model. Increasing VOC background concentrations result in less HNO_3 production because (R13)–(R14) and (R15)–(R16) outcompete (R3)–(R5) when the organic concentrations are high. At the same time, when VOC backgrounds are high, more organic nitrate is produced, and the total HNO_3 + organic nitrate is higher (Figure 11; using an organic nitrate yield of unity as a tracer for NO_3 reactions). In this model, monoterpenes dominate the VOC reactivity with NO_3 and monoterpene nitrates are always 67% or greater of the organic compounds formed. Peroxyacetyl nitrate (PAN) is always under 20% of the organic compounds formed, with the highest percentages falling when total organic production is low, so the overall PAN produced remains very low. All the organic compounds were varied simultaneously (e.g., high values for all starting compounds or low values for all starting compounds), so it is likely there are atmospheric conditions where acetaldehyde is high and monoterpenes are lower, resulting in relatively greater PAN production than in these model runs. In the southeast U.S. where monoterpene concentrations remain important throughout the winter (Hagerman et al., 1997; Xu et al., 2015), it is possible that organic nitrate formation will dominate over N_2O_5 chemistry and HNO_3 production throughout the area. Due to the lack of VOC measurements on this flight, we are unable to constrain this effect well for these conditions; the degree to which monoterpene chemistry is influenced by nitrate, radical oxidation in the southeastern U.S. in winter is an important current topic that may influence seasonal budgets for organic aerosol (Xu et al., 2015) and further wintertime research flights would address these topics.

5. Conclusions

Overnight removal of NO_x from power plant plumes is dependent on a number of conditions. The prominent controlling factor is N_2O_5 loss rate constant (and, relatedly, N_2O_5 uptake). With a low N_2O_5 loss rate constant, there is minimal conversion to HNO_3 , regardless of other factors. Mixing rate and O_3 background are also important factors; when the O_3 background is low, the chemistry of N_2O_5 formation does not progress as quickly. Additionally, when there is little mixing of the plume with background O_3 , the same occurs. In the plume from the Harlee Branch power plant, evaluated here, the low N_2O_5 uptake, coupled with low aerosol surface area, results in slow loss of N_2O_5 . This causes very little NO_x conversion to HNO_3 , and therefore, most NO_x will be reformed the next day. Finally, the fate of organic nitrates is an important factor. If organic nitrates are converted rapidly to a terminal product or directly deposited, their fate can be considered the same as HNO_3 formation, whereas if they reform NO_x , they cannot participate in NO_x removal.

Acknowledgments

The authors would like to thank the NSF-NCAR Research Aircraft Facility staff. Data are available from NCAR at http://data.eol.ucar.edu/master_list/?project=WINTER. The model algorithm used was developed in IGOR Pro and is available at <https://esrl.noaa.gov/csd/groups/csd7/measurements/2015winter/pubs/>. Funding for Fibiger was supported by NSF award 1433358.

References

- Anttila, T., Kiendler-Scharr, A., Tillmann, R., & Mentel, T. F. (2006). On the reactive uptake of gaseous compounds by organic-coated aqueous aerosols: Theoretical analysis and application to the heterogeneous hydrolysis of N_2O_5 . *The Journal of Physical Chemistry, A*, 110(35), 10435–10443. <https://doi.org/10.1021/jp062403c>
- Apel, E. C., Hornbrook, R. S., Hills, A. J., Blake, N. J., Barth, M. C., Weinheimer, A., ... Riemer, D. D. (2015). Upper tropospheric ozone production from lightning NO_x -impacted convection: Smoke ingestion case study from the DC3 campaign. *Journal of Geophysical Research: Atmospheres*, 120, 2505–2523. <https://doi.org/10.1002/2014JD022121>
- Atkinson, R., Winer, A. M., & Pitts, J. N. (1986). Estimation of night-time N_2O_5 concentrations from ambient NO_2 and NO_3 radical concentrations and the role of N_2O_5 in night-time chemistry. *Atmospheric Environment*, 20(2), 331–339. [https://doi.org/10.1016/0004-6981\(86\)90035-1](https://doi.org/10.1016/0004-6981(86)90035-1)
- Atkinson, R., Baulch, D. L., Cox, R. A., Crowley, J. N., Hampson, R. F., Hynes, R. G., ... Troe, J. (2004). Evaluated kinetic and photochemical data for atmospheric chemistry: Volume I—Gas phase reactions of O_x , HO_x , NO_x and SO_x species. *Atmospheric Chemistry and Physics*, 4(6), 1461–1738. <https://doi.org/10.5194/acp-4-1461-2004>
- Atkinson, R., Baulch, D. L., Cox, R. A., Crowley, J. N., Hampson, R. F., Hynes, R. G., ... Subcommittee, I. (2006). Evaluated kinetic and photochemical data for atmospheric chemistry: Volume II: Gas phase reactions of organic species. *Atmospheric Chemistry and Physics*, 6(11), 3625–4055. <https://doi.org/10.5194/acp-6-3625-2006>

- Bertram, T. H., & Thornton, J. A. (2009). Toward a general parameterization of N_2O_5 reactivity on aqueous particles: The competing effects of particle liquid water, nitrate and chloride. *Atmospheric Chemistry and Physics*, 9(21), 8351–8363. <https://doi.org/10.5194/acp-9-8351-2009>
- Bloomer, B. J., Vinnikov, K. Y., & Dickerson, R. R. (2010). Changes in seasonal and diurnal cycles of ozone and temperature in the eastern U.S. *Atmospheric Environment*, 44(21–22), 2543–2551. <https://doi.org/10.1016/j.atmosenv.2010.04.031>
- Brown, S. S., & Stutz, J. (2012). Nighttime radical observations and chemistry. *Chemical Society Reviews*, 41(19), 6405–6447. <https://doi.org/10.1039/C2CS35181A>
- Brown, S. S., Stark, H., & Ravishankara, A. R. (2003). Applicability of the steady state approximation to the interpretation of atmospheric observations of NO_3 and N_2O_5 . *Journal of Geophysical Research*, 108(D17), 4539. <https://doi.org/10.1029/2003JD003407>
- Brown, S. S., Dibb, J. E., Stark, H., Aldener, M., Vozella, M., Whitlow, S., ... Ravishankara, A. R. (2004). Nighttime removal of NO_x in the summer marine boundary layer. *Geophysical Research Letters*, 31, L07108. <https://doi.org/10.1029/2004GL019412>
- Brown, S. S., Neuman, J. A., Ryerson, T. B., Trainer, M., Dubé, W. P., Holloway, J. S., ... Ravishankara, A. R. (2006). Nocturnal odd-oxygen budget and its implications for ozone loss in the lower troposphere. *Geophysical Research Letters*, 33, L08801. <https://doi.org/10.1029/2006GL025900>
- Brown, S. S., Dubé, W. P., Osthoff, H. D., Stutz, J., Ryerson, T. B., Wollny, A. G., ... Ravishankara, A. R. (2007). Vertical profiles in NO_3 and N_2O_5 measured from an aircraft: Results from the NOAA P-3 and surface platforms during the New England Air Quality Study 2004. *Journal of Geophysical Research*, 112, D22304. <https://doi.org/10.1029/2007JD008883>
- Brown, S. S., Dubé, W. P., Fuchs, H., Ryerson, T. B., Wollny, A. G., Brock, C. A., ... Ravishankara, A. R. (2009). Reactive uptake coefficients for N_2O_5 determined from aircraft measurements during the Second Texas Air Quality Study: Comparison to current model parameterizations. *Journal of Geophysical Research*, 114, D00F10. <https://doi.org/10.1029/2008JD011679>
- Brown, S. S., Dubé, W. P., Peischl, J., Ryerson, T. B., Atlas, E., Warneke, C., ... Ravishankara, A. R. (2011). Budgets for nocturnal VOC oxidation by nitrate radicals aloft during the 2006 Texas Air Quality Study. *Journal of Geophysical Research*, 116, D24305. <https://doi.org/10.1029/2011JD016544>
- Brown, S. S., Dubé, W. P., Karamchandani, P., Yarwood, G., Peischl, J., Ryerson, T. B., ... Ravishankara, A. R. (2012). Effects of NO_x control and plume mixing on nighttime chemical processing of plumes from coal-fired power plants. *Journal of Geophysical Research*, 117, D07304. <https://doi.org/10.1029/2011JD016954>
- Brown, S. S., Thornton, J. A., Keene, W. C., Pszenny, A. A. P., Sive, B. C., Dubé, W. P., ... Wolfe, D. E. (2013). Nitrogen, Aerosol Composition, and Halogens on a Tall Tower (NACHTT): Overview of a wintertime air chemistry field study in the front range urban corridor of Colorado. *Journal of Geophysical Research: Atmospheres*, 118, 8067–8085. <https://doi.org/10.1002/jgrd.50537>
- Brown, S. S., Dubé, W. P., Tham, Y. J., Zha, Q., Xue, L., Poon, S., ... Wang, T. (2016). Nighttime chemistry at a high altitude site above Hong Kong. *Journal of Geophysical Research: Atmospheres*, 121, 2457–2475. <https://doi.org/10.1002/2015JD024566>
- Brown, S. S., An, H. J., Lee, M., Park, J. H., Lee, S. D., Fibiger, D. L., ... Min, K. E. (2017). Cavity enhanced spectroscopy for measurement of nitrogen oxides in the anthropocene: Results from the Seoul Tower during MAPS 2015. *Faraday Discussions*, 200, 529–557.
- Cazorla, M., Wolfe, G. M., Bailey, S. A., Swanson, A. K., Arkinson, H. L., & Hanisco, T. F. (2015). A new airborne laser-induced fluorescence instrument for in situ detection of formaldehyde throughout the troposphere and lower stratosphere. *Atmospheric Measurement Techniques*, 8(2), 541–552. <https://doi.org/10.5194/amt-8-541-2015>
- Darer, A. I., Cole-Filipiak, N. C., O'Connor, A. E., & Elrod, M. J. (2011). Formation and stability of atmospherically relevant isoprene-derived organosulfates and organonitrates. *Environmental Science & Technology*, 45(5), 1895–1902. <https://doi.org/10.1021/es103797z>
- Davis, J. M., Bhavsar, P. V., & Foley, K. M. (2008). Parameterization of N_2O_5 reaction probabilities on the surface of particles containing ammonium, sulfate, and nitrate. *Atmospheric Chemistry and Physics*, 8(17), 5295–5311. <https://doi.org/10.5194/acp-8-5295-2008>
- Day, D. A., Wooldridge, P. J., Dillon, M. B., Thornton, J. A., & Cohen, R. C. (2002). A thermal dissociation laser-induced fluorescence instrument for in situ detection of NO_2 , peroxy nitrates, alkyl nitrates, and HNO_3 . *Journal of Geophysical Research*, 107(D6), D000779. <https://doi.org/10.1029/2001JD000779>
- Dentener, F. J., & Crutzen, P. J. (1993). Reaction of N_2O_5 on tropospheric aerosols: Impact on the global distributions of NO_x , O_3 , and OH. *Journal of Geophysical Research*, 98(D4), 7149–7163. <https://doi.org/10.1029/92JD02979>
- Dubé, W. P., Brown, S. S., Osthoff, H. D., Nunley, M. R., Ciciora, S. J., Paris, M. W., ... Ravishankara, A. R. (2006). Aircraft instrument for simultaneous, in situ measurement of NO_3 and N_2O_5 via pulsed cavity ring-down spectroscopy. *The Review of Scientific Instruments*, 77(3), 034101. <https://doi.org/10.1063/1.2176058>
- Edwards, P. M., Aikin, K. C., Dube, W. P., Fry, J. L., Gilman, J. B., de Gouw, J. A., ... Brown, S. S. (2017). Transition from high- to low- NO_x control of night-time oxidation in the southeastern US. *Nature Geoscience*, 10(7), 490–495. <https://doi.org/10.1038/ngeo2976>, <https://www.nature.com/articles/ngeo2976> - supplementary-information
- Evans, M. J., & Jacob, D. J. (2005). Impact of new laboratory studies of N_2O_5 hydrolysis on global model budgets of tropospheric nitrogen oxides, ozone, and OH. *Geophysical Research Letters*, 32, L09813. <https://doi.org/10.1029/2005GL022469>
- Fuchs, H., Dubé, W. P., Ciciora, S. J., & Brown, S. S. (2008). Determination of inlet transmission and conversion efficiencies for in situ measurements of the nocturnal nitrogen oxides, NO_3 , N_2O_5 and NO_2 , via pulsed cavity ring-down spectroscopy. *Analytical Chemistry*, 80(15), 6010–6017. <https://doi.org/10.1021/ac8007253>
- Fuchs, H., Dubé, W. P., Lerner, B. M., Wagner, N. L., Williams, E. J., & Brown, S. S. (2009). A sensitive and versatile detector for atmospheric NO_2 and NO_x based on blue diode laser cavity ring-down spectroscopy. *Environmental Science & Technology*, 43(20), 7831–7836. <https://doi.org/10.1021/es902067h>
- Gaston, C. J., Thornton, J. A., & Ng, N. L. (2014). Reactive uptake of N_2O_5 to internally mixed inorganic and organic particles: The role of organic carbon oxidation state and inferred organic phase separations. *Atmospheric Chemistry and Physics*, 14(11), 5693–5707. <https://doi.org/10.5194/acp-14-5693-2014>
- Guo, H., Sullivan, A. P., Campuzano-Jost, P., Schroder, J. C., Lopez-Hilfiker, F. D., Dibb, J. E., ... Weber, R. J. (2016). Fine particle pH and the partitioning of nitric acid during winter in the northeastern United States. *Journal of Geophysical Research: Atmospheres*, 121, 10,355–10,376. <https://doi.org/10.1002/2016JD025311>
- Hagerman, L. M., Aneja, V. P., & Lonneman, W. A. (1997). Characterization of non-methane hydrocarbons in the rural southeast United States. *Atmospheric Environment*, 31(23), 4017–4038. [https://doi.org/10.1016/S1352-2310\(97\)00223-9](https://doi.org/10.1016/S1352-2310(97)00223-9)
- Hallquist, M., Wängberg, I., Ljungström, E., Barnes, I., & Becker, K.-H. (1999). Aerosol and product yields from NO_3 radical-initiated oxidation of selected monoterpenes. *Environmental Science & Technology*, 33(4), 553–559. <https://doi.org/10.1021/es980292s>
- Hegg, D., Hobbs, P. V., Radke, L. F., & Harrison, H. (1977). Reactions of ozone and nitrogen oxides in power plant plumes. *Atmospheric Environment*, 11(6), 521–526. [https://doi.org/10.1016/0004-6981\(77\)90069-5](https://doi.org/10.1016/0004-6981(77)90069-5)
- Hewitt, C. N. (2001). The atmospheric chemistry of sulphur and nitrogen in power station plumes. *Atmospheric Environment*, 35(7), 1155–1170. [https://doi.org/10.1016/S1352-2310\(00\)00463-5](https://doi.org/10.1016/S1352-2310(00)00463-5)

- Kercher, J. P., Riedel, T. P., & Thornton, J. A. (2009). Chlorine activation by N_2O_5 : Simultaneous, in situ detection of ClNO_2 and N_2O_5 by chemical ionization mass spectrometry. *Atmospheric Measurement Techniques*, 2(1), 193–204. <https://doi.org/10.5194/amt-2-193-2009>
- Lee, B. H., Lopez-Hilfiker, F. D., Mohr, C., Kurtén, T., Worsnop, D. R., & Thornton, J. A. (2014). An iodide-adduct high-resolution time-of-flight chemical-ionization mass spectrometer: Application to atmospheric inorganic and organic compounds. *Environmental Science & Technology*, 48(11), 6309–6317. <https://doi.org/10.1021/es500362a>
- Liu, F., Zhang, Q., Tong, D., Zheng, B., Li, M., Huo, H., & He, K. B. (2015). High-resolution inventory of technologies, activities, and emissions of coal-fired power plants in China from 1990 to 2010. *Atmospheric Chemistry and Physics*, 15(23), 13,299–13,317. <https://doi.org/10.5194/acp-15-13299-2015>
- Luria, M., Valente, R. J., Bairai, S., Parkhurst, W. J., & Tanner, R. L. (2008). Nighttime chemistry in the Houston urban plume. *Atmospheric Environment*, 42(32), 7544–7552. <https://doi.org/10.1016/j.atmosenv.2008.04.054>
- McLaren, R., Salmon, R. A., Liggio, J., Hayden, K. L., Anlauf, K. G., & Leaitch, W. R. (2004). Nighttime chemistry at a rural site in the Lower Fraser Valley. *Atmospheric Environment*, 38(34), 5837–5848. <https://doi.org/10.1016/j.atmosenv.2004.03.074>
- Peischl, J., Ryerson, T. B., Holloway, J. S., Parrish, D. D., Trainer, M., Frost, G. J., ... Fehsenfeld, F. C. (2010). A top-down analysis of emissions from selected Texas power plants during TexAQ5 2000 and 2006. *Journal of Geophysical Research*, 115, D16303. <https://doi.org/10.1029/2009JD013527>
- Ridley, B. A., Walega, J. G., Dye, J. E., & Grahek, F. E. (1994). Distributions of NO , NO_x , NO_y , and O_3 to 12 km altitude during the summer monsoon season over New Mexico. *Journal of Geophysical Research*, 99(D12), 25,519–25,534. <https://doi.org/10.1029/94JD02210>
- Riedel, T. P., Wagner, N. L., Dubé, W. P., Middlebrook, A. M., Young, C. J., Öztürk, F., ... Thornton, J. A. (2013). Chlorine activation within urban or power plant plumes: Vertically resolved ClNO_2 and Cl_2 measurements from a tall tower in a polluted continental setting. *Journal of Geophysical Research: Atmospheres*, 118, 8702–8715. <https://doi.org/10.1002/jgrd.50637>
- Rindelaub, J. D., Borca, C. H., Hostetler, M. A., Slade, J. H., Lipton, M. A., Slipchenko, L. V., & Shepson, P. B. (2016). The acid-catalyzed hydrolysis of an α -pinene-derived organic nitrate: Kinetics, products, reaction mechanisms, and atmospheric impact. *Atmospheric Chemistry and Physics*, 16(23), 15,425–15,432. <https://doi.org/10.5194/acp-16-15425-2016>
- Roberts, J. M., Osthoff, H. D., Brown, S. S., & Ravishankara, A. R. (2008). N_2O_5 oxidizes chloride to Cl_2 in acidic atmospheric aerosol. *Science*, 321(5892), 1059–1059. <https://doi.org/10.1126/science.1158777>
- Roberts, J. M., Osthoff, H. D., Brown, S. S., Ravishankara, A. R., Coffman, D., Quinn, P., & Bates, T. (2009). Laboratory studies of products of N_2O_5 uptake on Cl-containing substrates. *Geophysical Research Letters*, 36, L20808. <https://doi.org/10.1029/2009GL040448>
- Russo, R. S., Zhou, Y., White, M. L., Mao, H., Talbot, R., & Sive, B. C. (2010). Multi-year (2004–2008) record of nonmethane hydrocarbons and halocarbons in New England: Seasonal variations and regional sources. *Atmospheric Chemistry and Physics*, 10(10), 4909–4929. <https://doi.org/10.5194/acp-10-4909-2010>
- Ryerson, T. B., Buhr, M. P., Frost, G. J., Goldan, P. D., Holloway, J. S., Hübler, G., ... Fehsenfeld, F. C. (1998). Emissions lifetimes and ozone formation in power plant plumes. *Journal of Geophysical Research*, 103(D17), 22,569–22,583. <https://doi.org/10.1029/98JD01620>
- Ryerson, T. B., Trainer, M., Holloway, J. S., Parrish, D. D., Huey, L. G., Sueper, D. T., ... Fehsenfeld, F. C. (2001). Observations of ozone formation in power plant plumes and implications for ozone control strategies. *Science*, 292(5517), 719–723. <https://doi.org/10.1126/science.1058113>
- Strapp, J. W., Leaitch, W. R., & Liu, P. S. K. (1992). Hydrated and dried aerosol-size-distribution measurements from the particle measuring systems FSSP-300 Probe and the Deiced PCASP-100X Probe. *Journal of Atmospheric and Oceanic Technology*, 9(5), 548–555. [https://doi.org/10.1175/1520-0426\(1992\)9<548>2.0.CO;2](https://doi.org/10.1175/1520-0426(1992)9<548>2.0.CO;2)
- Turner, B. D. (1994). *Atmospheric Dispersion Estimates*. Boca Raton, FL: Lewis Publishers.
- Wagner, N. L., Dubé, W. P., Washenfelder, R. A., Young, C. J., Pollack, I. B., Ryerson, T. B., & Brown, S. S. (2011). Diode laser-based cavity ring-down instrument for NO_3 , N_2O_5 , NO , NO_2 and O_3 from aircraft. *Atmospheric Measurement Techniques*, 4(6), 1227–1240. <https://doi.org/10.5194/amt-4-1227-2011>
- Wagner, N. L., Riedel, T. P., Young, C. J., Bahreini, R., Brock, C. A., Dubé, W. P., ... Brown, S. S. (2013). N_2O_5 uptake coefficients and nocturnal NO_2 removal rates determined from ambient wintertime measurements. *Journal of Geophysical Research: Atmospheres*, 118, 9331–9350. <https://doi.org/10.1002/jgrd.50653>
- Warneke, C., de Gouw, J. A., Holloway, J. S., Peischl, J., Ryerson, T. B., Atlas, E., ... Parrish, D. D. (2012). Multiyear trends in volatile organic compounds in Los Angeles, California: Five decades of decreasing emissions. *Journal of Geophysical Research*, 117, D00V17. <https://doi.org/10.1029/2012JD017899>
- Washenfelder, R. A., Wagner, N. L., Dube, W. P., & Brown, S. S. (2011). Measurement of atmospheric ozone by cavity ring-down spectroscopy. *Environmental Science & Technology*, 45(7), 2938–2944. <https://doi.org/10.1021/es103340u>
- Wild, R. J., Edwards, P. M., Dubé, W. P., Baumann, K., Edgerton, E. S., Quinn, P. K., ... Brown, S. S. (2014). A measurement of total reactive nitrogen, NO_y , together with NO_2 , NO , and O_3 via cavity ring-down spectroscopy. *Environmental Science & Technology*, 48(16), 9609–9615. <https://doi.org/10.1021/es501896w>
- Xu, L., Suresh, S., Guo, H., Weber, R. J., & Ng, N. L. (2015). Aerosol characterization over the southeastern United States using high-resolution aerosol mass spectrometry: Spatial and seasonal variation of aerosol composition and sources with a focus on organic nitrates. *Atmospheric Chemistry and Physics*, 15(13), 7307–7336. <https://doi.org/10.5194/acp-15-7307-2015>
- Zaveri, R. A., Berkowitz, C. M., Brechtel, F. J., Gilles, M. K., Hubbe, J. M., Jayne, J. T., ... Worsnop, D. R. (2010). Nighttime chemical evolution of aerosol and trace gases in a power plant plume: Implications for secondary organic nitrate and organosulfate aerosol formation, NO_3 radical chemistry, and N_2O_5 heterogeneous hydrolysis. *Journal of Geophysical Research*, 115, D12304. <https://doi.org/10.1029/2009JD013250>